Adsorption of Perfluorinated Compounds on Thin-Film Composite Polyamide Membranes

Young-Nam Kwon,[1] Kaimin Shih,[2] Chuyang Tang,[3] James O. Leckie[4]

[1]*School of Urban and Environmental Engineering, Ulsan National Institute of Science and Technology (UNIST), Korea 689-798*
[2]*Department of Civil Engineering, University of Hong Kong, Pokfulam Road, Hong Kong*
[3]*School of Civil and Environmental Engineering, Nanyang Technological University, Singapore 639798*
[4]*Environmental Engineering and Science, Department of Civil and Environmental Engineering, Stanford University, Stanford, California 94305-4020*

Received 31 March 2011; accepted 4 July 2011
DOI 10.1002/app.35182
Published online 11 October 2011 in Wiley Online Library (wileyonlinelibrary.com).

ABSTRACT: The adsorption behavior of perfluorinated compounds (PFCs), of various chain lengths and two different functional groups, on widely used thin-film composite polyamide membranes has been investigated. Three commercially available polyamide membranes and two classes of PFCs were evaluated: Dow-Filmtech BW30, NF90, and NF270 membranes; perfluorosulfonic and perfluoroalkanoic acid with 5, 7, 9, and 11 carbon atoms. The adsorption of PFCs on the membranes strongly depended on the active skin-top layer material of the membranes, solution chemistry, and structure of PFCs. The piperazine based NF270 membrane showed higher adsorption of PFCs compared to BW30 and NF90 membranes (FT-30 type membranes). The BW30 membrane, which has a coating layer of aliphatic carbons and hydroxyl groups on the surface of the polyamide substrate, had less interaction with PFCs than the NF90 polyamide membrane had. The adsorption of PFCs increased with increasing ionic strength, decreasing pH, and in divalent ion solutions. PFCs with longer chain lengths and more hydrophobic functional groups showed more attractive interactions with thin-film composite membranes and, thus, greater adsorption on the membranes.
 J Appl Polym Sci 124: 1042–1049, 2012

Key words: adsorption; polyamide; membrane; perfluorinated compounds

INTRODUCTION

Perfluorinated compounds (PFCs) are used in a wide variety of consumer and industrial products due to their stability, which result from strong C—F bonds and effective shielding of carbons by the highly electronegative fluorines.[1] PFCs are compounds which do not break down chemically or biologically in the environment. PFCs are widely used in cleaning products, fire-fighting foams, hydraulic fluids, metal plating solutions, and photolithographic resist formulas for their surface activity and persistence.[2] However, PFCs are globally distributed and have been reported in air, drinking water, and wildlife including fish, birds, marine mammals, and even humans due to their persistence and bioaccumulative characteristics.[3–7]

Controlling the release of PFCs has become a major issue in industries that use the compounds and demands to treat wastewater containing PFCs are increasing. Activated carbon (AC) can remove PFCs (60–90% removal with powdered activated carbon) in a short exposure time promoted by hydrophobic effects on the AC.[8,9] Various research has shown that membrane processes are also feasible for treating PFC-contaminated wastewater. Perfluorooctanesulfonic acid (PFOS) filtration tests with commercially available reverse osmosis (RO) and nanofiltration (NF) membranes demonstrated more than 99 and 90% rejection, respectively, and the rejection of PFCs could be improved by adjusting the pH of the feed solution.[10–14] Tasi et al.[15] revealed that even microfiltration process can remove about 70% of PFCs by applying a direct electrical field across the membrane. However, the flux performance of membranes gradually deteriorates due to PFOS accumulation with filtration time. For membrane technologies to be economically feasible for removal of PFCs, a fundamental understanding of the adsorption behaviors of PFCs that cause subsequent membrane fouling is required.

Thin-film composite polyamide membranes and cellulose acetate membranes are the main types of RO and NF membranes, but thin-film composite

Correspondence to: Y.-N. Kwon (kwonyn@unist.ac.kr).
Contract grant sponsor: Basic Science Research Program, National Research Foundation of Korea, Ministry of Education, Science and Technology; contract grant number: 2010-0015988.
Contract grant sponsor: 2009 Research Fund of UNIST (Ulsan National Institute of Science and Technology.

polyamide membranes have been displacing cellulose acetate membranes due to their outstanding stabilities. Commercially available thin-film composite polyamide RO and NF membranes can be categorized[16–18] into three groups (1): typical polyamide membranes, (2) polyamide membranes with a coating layer composed of aliphatic carbons and hydroxyl functional groups, (3) piperazine-based membranes. These membranes have different surface chemical and morphological properties, indicating that the membranes may have different degrees of interaction with PFCs and different fouling tendencies.

The objectives of this work are to investigate the adsorption behavior of PFCs on widely used polyamide membranes at various solution chemistries and to investigate the effect of the surface properties of polyamide membranes and the structures of the PFCs on the interactions between the membranes and PFCs. Physicochemical surface properties of the membranes were investigated using streaming potential analysis, attenuated total reflection Fourier transform infrared spectroscopy (ATR-FTIR), and atomic force microscopy (AFM). Thin-film composite polyamide membranes (BW30, NF90, and NF270) were used and perfluorosulfonic and perfluoroalkanoic acid PFCs with 5, 7, 9, and 11 carbon atoms were evaluated.

MATERIALS AND METHODS

Chemicals

Perfluorooctanesulfonic acid (PFOS, 100%, $C_8F_{17}SO_3H$) was provided by AZ Electronic Materials USA (Sommerville, NJ) through SEMATECH (Austin, TX). Perfluoropentanoic acid (PFPeA, 98%, C_4F_9COOH) was purchased from Alfa Aesar (Ward Hill, MA); perfluoroheptanoic acid (PFHpA, 99%, $C_6F_{13}COOH$), perfluorononanoic acid (PFNA, 97%, $C_8F_{17}COOH$), and perfluoroundecanoic acid (PFUnA, 95%, $C_{10}F_{21}COOH$) were purchased from Aldrich (St. Louis, MO). Stock solutions of PFCs (1 g/L) were prepared by dissolution in methanol, and stored at 4°C. PFC solutions for the adsorption experiments were prepared by dilution of stock solutions with Milli-Q water. Milli-Q water from a MilliPore system (Billerica, MA) has a resistivity of 18.2 MΩ-cm^{-1}. Reagent-grade sodium chloride, magnesium sulfate, sodium hydroxide, and hydrochloric acid were purchased from Fisher Scientific (Santa Clara, CA).

Thin-film composite membranes

We have used three commercially available FilmTec© membranes (BW30, NF90, and NF270) as representative thin-film composite polyamide membranes. The BW30 and NF90 membranes are aromatic FT-30 type polyamide membranes, produced by interfacial polymerization of diamine and acyl chloride. The NF270 membrane is a semiaromatic piperazine-based polyamide membrane. All membrane samples were shipped dry from the manufacturer, so they were stored dry in a dark chamber at 4°C.

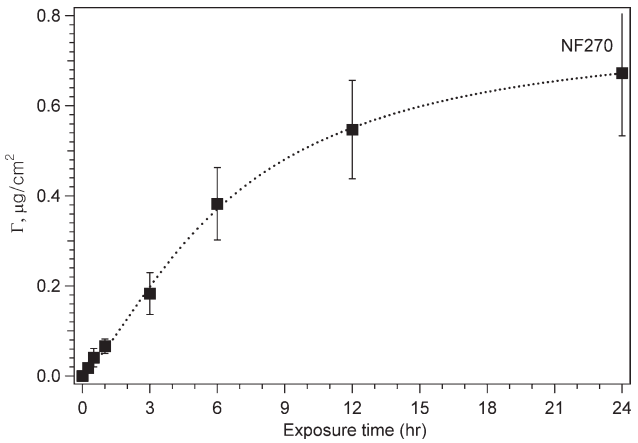

Figure 1 Kinetics of PFOS adsorption on NF 270 membrane C_o (PFOS concentration in soaking bath) = 1 mg/L; pH 5.3; ionic strength = 17.1 m*M* (NaCl); adsorption carried out for 24 h; 200 rpm stirring speed. Γ = amount adsorbed per membrane surface area (g/cm^2).

Static adsorption

Static adsorption experiments were carried out in six 400-mL stirred Amicon cells (model 8400) at room temperature. Prior to the adsorption test, each membrane sample was soaked in Milli-Q water for 2 days. The soaked membranes with nominal membrane areas of 41.8 cm^2 were placed in the cells, and only the active side of the membranes was exposed to 1 ppm PFC solutions for the exposure time. The ionic strengths of monovalent and divalent ion solutions were 17.1 m*M* prepared from NaCl and $MgSO_4$, respectively. The PFC solutions for the six cells were mechanically stirred at 200 rpm. After the membranes had been in contact with the solution for the required time, the membranes were removed and gently rinsed with flowing Milli-Q water. The adsorbed PFCs were chemically desorbed by immersing the rinsed membranes in 50 mL of 50% methanol for at least 48 h. After the PFCs were desorbed from the membranes, the extent of adsorption on the membranes was determined using LC/MS/MS. Each data point displayed in Figures 1, 5, 6 and Tables I and II represent an average of six replicates.

PFCs quantification

The aqueous PFC samples were analyzed by high-performance liquid chromatography (HPLC) with a

TABLE I
Amount of PFCs Absorbed on Thin-Film Composite BW30, NF90, and NF270 Membranes[a]

Ionic strength (ppm)	PFOS (pg/cm^2)			PFNA (pg/cm^2)		
	BW30	NF90	NF270	BW30	NF90	NF270
10	22.37 ± 8.52	123.61 ± 24.82	166.71 ± 13.27	3.96 ± 1.30	50.06 ± 12.09	72.390 ± 5.48
100	23.35 ± 5.76	142.79 ± 31.97	306.26 ± 31.55	10.57 ± 1.96	51.85 ± 10.25	99.10 ± 11.40
1000	35.46 ± 18.33	156.78 ± 42.04	672.96 ± 139.68	15.58 ± 14.84	56.06 ± 22.55	312.24 ± 53.67

[a] Adsorption under the condition of various ionic strength at pH 5.
C_o (PFCs concentration in soaking bath) =1 mg/L; pH 5.3; adsorption carried out for 24 h; 200 rpm stirring speed. Γ = amount adsorbed per membrane surface area (pg/cm^2). Target ionic strengths were prepared with NaCl.

Shimadzu LC system (LC10ADvp pumps controlled by a SCL10Avp controller (Columbia, MD)) coupled to a Sciex API 3000 triple quadrupole mass spectrometer (MDS Sciex, Ontario). Quantification was performed with 1 ppb (μg/L) of ^{13}C PFOS (for perfluorooctanesulfonate) or ^{13}C PFNA (for perfluoroalkanoic acids) purchased from Wellington Laboratories (Guelph, ON) as internal standards. A 6-point calibration curve spanning the 1–50 ppb range was developed at the beginning and the end of each analysis batch. Solvent blanks were used to monitor instrument background; 5 ppb standards were used to monitor the validity of the calibration after every sixth sample.

Methods of characterization

Streaming potential measurement

Membrane zeta potentials were measured using a BI-EKA streaming potential analyzer (Brookhaven, NY) with NaCl electrolyte solutions. EKA uses Ag/AgCl electrodes to measure the potential difference (ΔU) between two electrodes and a differential pressure sensor to monitor pressure difference (ΔP) at the two electrodes. The zeta potential was calculated from the quotient $\Delta U/\Delta P$ using the Helmholtz-Smoluchowski equation and the Fairbrother-Mastin approach. The streaming potentials were measured at pH of 3, 5.3, and 11. Results shown for each pH represent an average of 12 measurements for each specific pH, for two replicates from the experiment matrix.

Attenuated total reflection—Fourier transform infrared spectroscopy (ATR-FTIR)

ATR-FTIR spectra were recorded on a Magna 550 FTIR spectrometer (Thermo Electron Corp. Madison, WI). As an internal reflection element, a Ge crystal (45° single-reflection germanium ThunderDome internal reflection element, Thermo Spectra-Tech, Madison, WI) was used. When pressed tightly against the membranes, the germanium ATR element samples a circular disk of about 2 mm in diameter. Eighteen replicate ATR-FTIR spectra were obtained for each membrane type, with each spectra averaged from 128 scans collected from 650 to 4000 cm^{-1} at 2 cm^{-1} resolution. These spectra were subsequently corrected for the wavelength-dependent penetration depth and background subtraction with GRAMS/AI (version 7.02) software (Thermo Galactic, Salem, NH).

Atomic force microscope (AFM)

A nanoscope IV (Digital Instruments, CA) was used to examine the surface topography of wet membranes. Surface topography was investigated in contact mode in a wet cell.

RESULTS AND DISCUSSION

The time-dependent adsorption of PFOS onto a NF270 composite membrane is shown in Figure 1, where Γ is the mass adsorbed (μg) per membrane surface area (cm^2). The three-dimensional surface

TABLE II
Amount of PFCs Absorbed on Thin-Film Composite BW30, NF90, and NF270 Membranes[a]

pH	PFOS (pg/cm^2)			PFNA (pg/cm^2)		
	BW30	NF90	NF270	BW30	NF90	NF270
3	43.83 ± 17.68	641.818 ± 145.134	1286.38 ± 119.108	28.65 ± 17.34	516.72 ± 79.22	312.24 ± 53.67
5.3	35.46 ± 18.33	156.783 ± 42.035	672.963 ± 139.679	15.58 ± 14.84	56.06 ± 22.55	310.09 ± 54.26
11	20.377 ± 5.931	72.826 ± 25.396	536.216 ± 108.343	7.30 ± 2.78	39.80 ± 15.57	156.95 ± 40.48

[a] Adsorption under the condition of various pH values at ionic strength of 17.1 m*M* (NaCl).
C_o (PFCs concentration in soaking bath) =1 mg/L; ionic strength = 17.1 m*M* (NaCl); adsorption carried out for 24 h; 200 rpm stirring speed. Γ = amount adsorbed per membrane surface area (pg/cm^2).

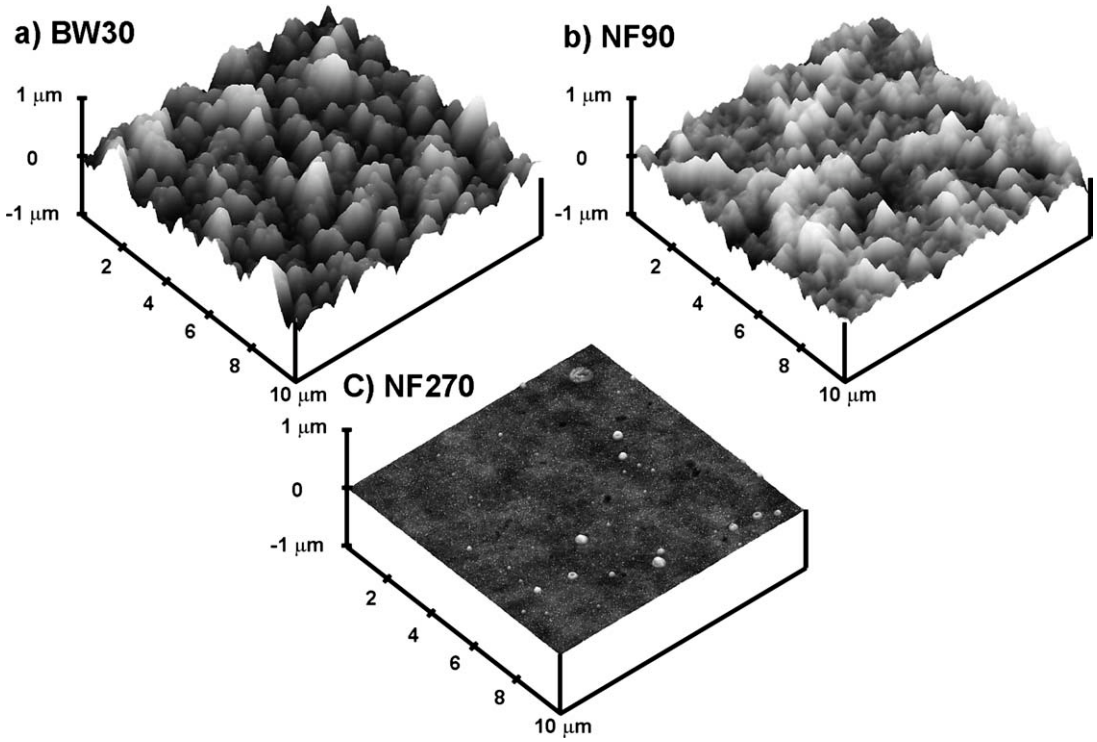

Figure 2 AFM images (10 × 10 μm^2) of the active surface layer of virgin BW30, NF90, and NF270 membranes. Surface area of BW30, NF90, and NF270 are 129 ± 8 μm^2, 130 ± 4 μm^2, 102 ± 1 μm^2, respectively.

area of the membrane was used for the calculation of mass per unit area. The three-dimensional area was obtained by AFM image analysis, summing the area of all of the triangles formed by three adjacent data points in the image (Fig. 2). The amount of PFOS adsorbed on the membrane from aqueous solution increased exponentially at early exposure times, and then the adsorbed mass became almost constant beyond 24 h, indicating that the membrane approached equilibrium with the PFOS solution. The rate of PFOS adsorption on the NF270 membrane is proportionate to the number of reaction sites on the membrane and the number of PFOS molecules. When we assume that the reaction rate depends only on the number of membrane reaction sites (because the concentration change of the PFOS molecules before and after exposure to the membranes was less than 10% in this research) and that the adsorption reaction comes to a state of equilibrium as time increases indefinitely, the mass (Γ) adsorbed on the membrane surface is expressed as a function of time.

$$\Gamma = \Gamma_e[1 - e^{-k\,t}] \quad (1)$$

where Γ_e is the maximum mass that can be adsorbed on the membrane when the adsorption reaction reaches equilibrium and k is a rate constant (t^{-1}). Values for Γ_e and k can be found by graphing adsorption versus time, as in Figure 1. When the initial concentration of PFOS was 1 ppm, the values for Γ_e and k were 0.724 $\mu g/cm^2$ and 0.1152 h^{-1}, respectively. The correlation coefficient for the experimental data and the data from eq. (1) was 0.9985. PFOS adsorption on the NF270 membrane was explained well by the first-order reversible reaction model. According to Manne et al.,[19] the adsorption of ionic surfactants around the critical micelle concentration (cmc) on a substrate plane is a two-step process. Ionic surfactants adsorb on the surface establishing a monolayer structure at low concentrations, and then hemimicelles grow on the monolayer serving as a template, forming cylindrical, half-cylindrical, or half-spherical shapes depending on the surfaces.[19–26] However, the two-step adsorption behavior was not observed in this research because the PFC concentrations used ware much lower than the cmc.

Tables I and II show the static adsorption of PFOS and PFNA on BW30, NF90, and NF270 composite polyamide membranes as functions of ionic strength and pH. Adsorption of PFOS and PFNA increased with increasing ionic strength and decreasing pH. Increased adsorption at higher ionic strengths is attributed to the decrease in repulsive interactions between similarly charged membranes and PFCs. PFOS and PFNA exist in anionic form at pH 5.3, because pKa values of PFOS and PFNA are expected to be less than 1 and around 3.5, respectively,.[27,28],

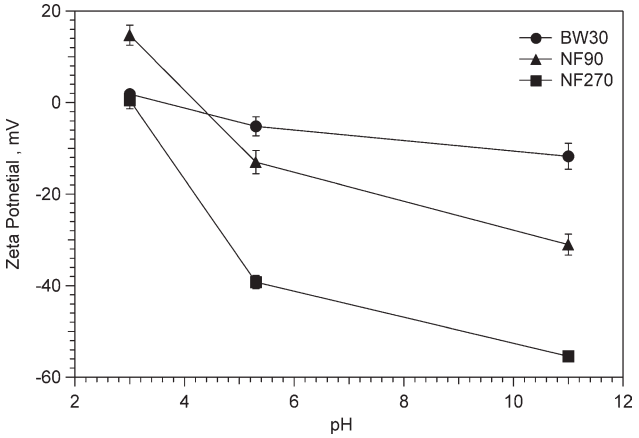

Figure 3 Zeta potential of virgin BW30, NF90, and NF270 membranes.

$$C_8F_{17}SO_3H \leftrightarrow C_8F_{17}SO_3H^- + H^+, \text{pKa} = \text{less than 1} \quad (2)$$

$$C_8F_{17}COOH \leftrightarrow C_8F_{17}COO^- + H^+, \text{pKa} = \text{around 3.5} \quad (3)$$

BW30, NF90, and NF270 membranes have negative zeta potentials at pH 5.3 (Fig. 3). Increasing ionic strength screens the electrical double-layer repulsion between negatively charged compounds and membranes, permitting closer packing of PFOS and PFNA on membrane surfaces. The more negatively charged NF270 composite membrane, which can have a greater screening effect, showed a greater increase of adsorption with increasing ionic strength compared to the others, less negatively charged NF90 and BW30 membranes.

The higher adsorption at lower pH is also attributed to decreased repulsive interactions between PFCs and membranes because the membranes have less negative zeta potential at lower pH (Fig. 4). It is interesting to note that the adsorption of PFNA on NF 90 at pH 3 was higher than on NF270 at pH 3. pKa values of surfactants with the same functional group and the same type of alkyl group depend on chain length, and perfluorooctanoic acid (C_7F_{15} COOH) and perfluorodecanoic acid ($C_9F_{19}COOH$) have pKa values between 2.5 and 3.5.[1,28,29] Therefore, the pKa value of PFNA ($C_8F_{17}COOH$) is expected to be around pH 3. At pH 3, PFNA exhibited both protonated and deprotonated forms and the NF90 membrane has a net positive charge. As a result of the attractive interaction between deprotonated PFNA and the positively charged NF90 membrane, the adsorption of PFNA on NF90 at pH 3 was higher than on the neutral NF270 membrane.

The extent of PFOS adsorption on each membrane was higher than comparable PFNA adsorption. PFOS and PFNA are surfactants composed of the same hydrophobic alkyl group (C_8F_{17}) but different hydrophilic functional groups (SO_3^- for PFOS and COO^- for PFNA). Surfactant adsorption is initially driven by repulsion of the surfactant from the aqueous solution.[30] The higher adsorption of PFOS compared to PFNA seems to be due to easy migration of

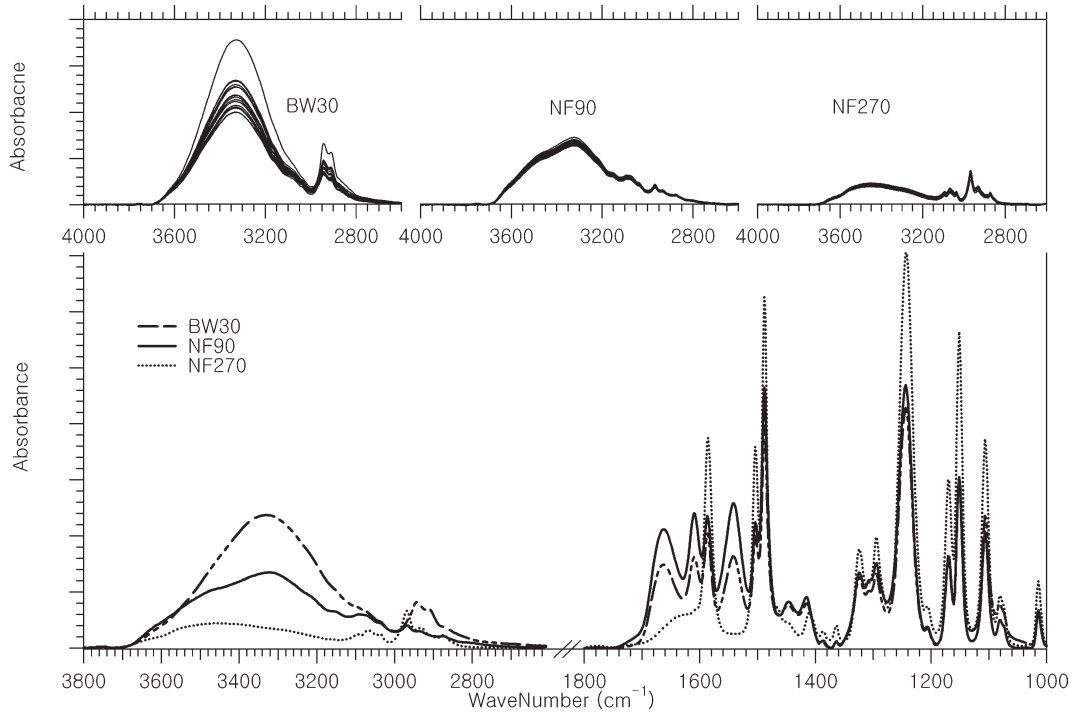

Figure 4 ATR-FTIR absorption spectra of virgin BW30, NF90, and NF270 membranes. (Top) Eighteen replicate ATR-FTIR spectra of each type of membrane. (Bottom) Average of 18 spectra for each type membrane.

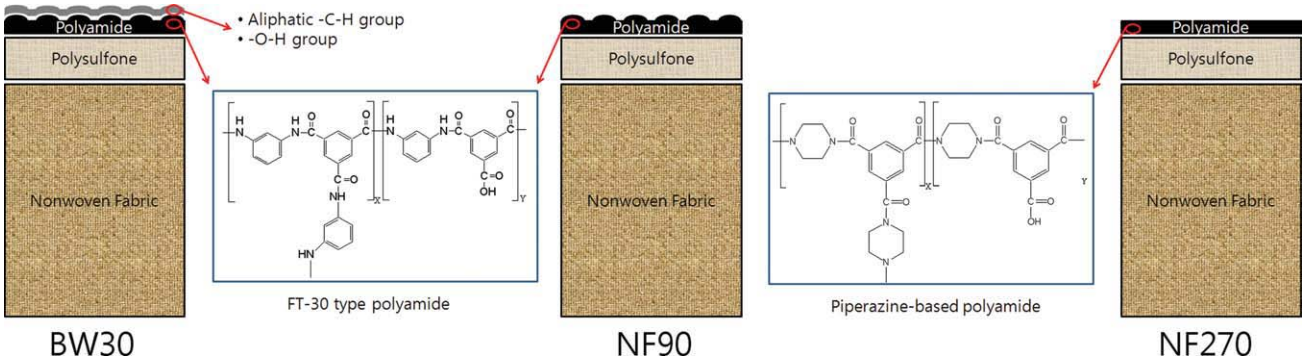

Figure 5 Schematic crosssection of BW30, NF90, and NF270 membranes and chemical structures of their active layers. [Color figure can be viewed in the online issue, which is available at wileyonlinelibrary.com.]

PFOS to the membrane surface from the aqueous solution caused by the lower hydrophilicity of sulfonate compared to carboxylate.[31]

Furthermore, Tables I and II show that the adsorption of PFOS and PFNA on composite membranes is strongly dependent on the material composing the active membrane layers. The chemical nature of the active layers of the BW30, NF90, and NF270 membranes was investigated using ATR-FTIR (Fig. 4). The NF90 membrane showed two bands at 3470 cm^{-1} and 3330 cm^{-1} corresponding to free and hydrogen-bonded NH stretching vibration modes, respectively,.[32,33] Small peaks above 3000 cm^{-1} were characteristic of the aromatic =C—H stretching mode.[34] The BW30 membrane exhibited a broad band centered around 3300 cm^{-1} corresponding to the O—H stretching vibration and peaks below 3000 cm^{-1} that correspond to the aliphatic C—H stretching vibration. The absorption frequencies of O—H and aliphatic C—H stretching vibration of BW30 membranes suggest that the BW30 membrane has an active layer containing both O—H and aliphatic C—H groups. NF90 and BW30 membranes were characterized by peaks exhibiting C=O stretching (amide I at 1663 cm^{-1}) and *N*—H bending (amide II at 1541 cm^{-1}) modes.[33–35] The peaks at 1587, 1504, and 1488 cm^{-1}, which were also observed for the polysulfone sublayer, were attributed to the aromatic ring C—C stretching motion.[36,37] The absorbance intensities of amide I and II peaks and peaks associated with C—C stretching vibration in the BW30 membrane were lower than those in the NF90 membrane. The existence of amide I and II peaks and the lower intensities of the amide bonds and polysulfone C—C peaks in BW30 could be explained by the existence of a coating on the polyamide layer, consistent with previous discussions of the peak region around 3000 cm^{-1}. Eighteen replicates of the BW30 membrane above 3000 cm^{-1} showed larger scattered spectra compared to the NF90 and NF270 membranes. This is also attributed to the existence of a nonuniformly deposited coating layer. The coating layer decreased the negative zeta potential of the membrane by blocking surface charge (Fig. 3) and improved hydrophilicity of the membrane, as reported earlier.[17] Lower peak intensities around 3300 cm^{-1}, 1663 cm^{-1}, and 1541 cm^{-1} in NF270 show that the membrane is not a typical FT-30 type polyamide but rather a piperazine-based polyamide membrane. Schematic cross section of BW30, NF90, and NF270 membranes and chemical structures of their active layers are shown in Figure 5. The NF270 piperazine-based membranes showed higher adsorption of PFOS and PFNA compounds compared to BW30 and NF90 membranes (FT-30 type membranes). The BW30 polyamide membrane, which has a coating layer of aliphatic carbons and hydroxyl groups, had less interaction with PFOS and PFNA than the NF90 membrane, even if both the BW30 and NF90 are known as the same polyamide type membranes.

Figure 6 shows the effect of divalent ions on the adsorption of PFNA on thin-film composite

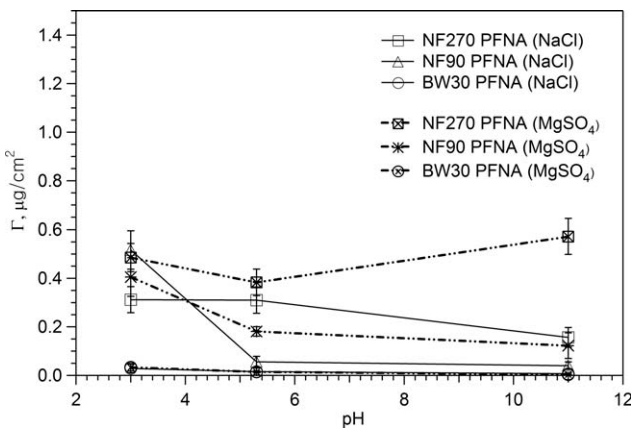

Figure 6 Adsorption of PFNA on thin-film composite BW30, NF90, and NF270 membranes in monovalent and divalent ion solutions. C_o (PFOS concentration in soaking bath) = 1 mg/L; ionic strength = 17.1 m*M* (NaCl or $MgSO_4$); adsorption carried out for 24 h; 200 rpm stirring speed. Γ = amount adsorbed per membrane surface area ($\mu g/cm^2$).

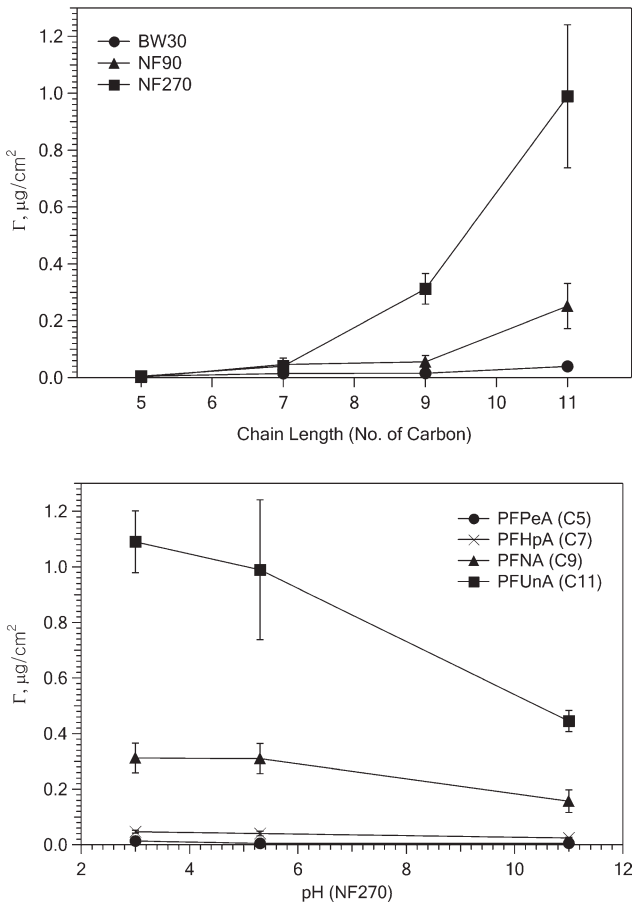

Figure 7 Static adsorption of PFCs on thin-film composite BW30, NF90, and NF270 membranes as a function of chain length at pH 5.3 (top), and adsorption on NF270 as a function of pH (bottom). C_o (PFOS concentration in soaking bath) = 1 mg/L; ionic strength = 17.1 m*M* (NaCl); adsorption carried out for 24 h; 200 rpm stirring speed. Γ = amount adsorbed per membrane surface area (μg/cm^2)

membranes. The ionic strengths of monovalent and divalent ion solutions used in this research were 17.1 m*M* (equivalent to 1000 ppm NaCl). Divalent ions in the solution caused increased PFNA adsorption (except on NF90 at pH 3). The increase of adsorption is attributed to a "Mg^{2+} bridge" between the negatively charged membrane and PFNA, which leads to more adsorption on the membranes.[38] Decreased PFNA adsorption on NF90 at pH 3 in divalent ion solutions resulted from decreased attractive interaction between the oppositely charged membrane and PFNA. Adsorption of SO_4^{2-} on the positively charged NF90 membrane at pH 3 yields a negative charge on the membrane and causes repulsive interactions between negative PFNA and the membrane surface.

Figure 7 shows the effect of hydrophobic alkyl group chain lengths on adsorption of perfluoroalkanoic acid with 5, 7, 9, and 11 carbon atoms. Increased alkyl chain length increased adsorption on thin-film composite membranes, because the free energy associated with repulsion of the PFCs from aqueous solution decreases and the dispersion forces between the compounds and membrane increase with increasing chain length.[39] An effect similar to that of chain length was observed for PFC sorption by sediment organic matter.[40] The adsorption of PFCs depended on membrane type and pH, as discussed in Tables I and II. The BW30 polyamide membrane with a hydrophilic-neutral coating layer had lower adsorption of PFCs than NF90 and piperazine-based NF270 membranes had higher adsorption. Adsorption of PFCs on the membranes decreased with increasing pH, which is attributed to the increased repulsive interactions between PFCs and membranes, because the membranes contain a more negative zeta potential at higher pH.

CONCLUSIONS

Adsorption behaviors of various PFCs on three different types of polyamide membranes were systematically investigated with respect to the physicochemical properties of membranes, structure of PFCs, and solution chemistry.

Adsorption of PFOS followed a first-order reversible reaction model approaching equilibrium, increasing exponentially in the early stages of exposure and then becoming constant beyond 24 h. Adsorption of PFOS and PFNA increased with increasing ionic strength and decreasing pH due to decreased electrostatic repulsion between membrane surfaces and PFCs. The presence of divalent ions in solution caused increased PFC adsorption, except on oppositely charged membranes. The extent of PFOS adsorption on each membrane was higher than the extent of comparable PFNA adsorption. This is attributed to the easy migration of PFOS, which contains more hydrophobic functional groups, to the membrane surface from the aqueous solution compared to PFNA. PFCs adsorption on thin-film composite membranes strongly depended on the material composing the active layer of the membranes. NF270 piperazine-based membranes showed higher adsorption of PFOS and PFNA compounds compared to BW30 and NF90 membranes (FT-30 type membranes). The BW30 polyamide membrane, which has an aliphatic carbon and hydroxyl group coating layer, had less interaction with PFOS and PFNA than the NF90 polyamide membrane. Polyamide membrane adsorption of PFC increased with increasing compound chain length due to the decrease of free energy associated with repulsion of PFCs from aqueous solution and/or increasing dispersion forces between membranes and PFCs with increasing PFC chain length.

This research shows that adsorption behavior of PFCs on commercial thin-film composite polyamide membranes depends on the electrostatic interaction of membranes and PFCs as functions of the applied solution chemistry, the active layer material of the membranes, and the PFC chain length/functional group.

References

1. Kissa, E. Fluorinated Surfactants and Repellents; CRC: Boca Raton, 2001.
2. Brooke, D.; Footitt, A.; Nwaogu, T. A. Environmental risk evaluation report: Perfluoroocatnesulphonate, Building Research Establishment, Ltd; Risk and Policy Analysts Ltd., 2004.
3. Giesy, J. P.; Kannan, K. Environ Sci Technol 2001, 35, 1339.
4. Hansen, K. J.; Clemen, L. A.; Ellefson, M. E.; Johnson, H. O. Environ Sci Technol 2001, 35, 766.
5. Jones, P. D.; Hu, W. Y.; De Coen, W.; Newsted, J. L.; Giesy, J. P. Environ Toxicol Chem 2003, 22, 2639.
6. Kunacheva, C.; Fujii, S.; Tanaka, S.; Boontanon, S. K.; Poothong, S.; Wongwatthana, T.; Shivakoti, B. R. J Water Supply Res Technol Aqua 2010, 59, 345.
7. Tomy, G. T.; Budakowski, W.; Halldorson, T.; Helm, P. A.; Stern, G. A.; Friesen, K.; Pepper, K.; Tittlemier, S. A.; Fisk, A. T. Environ Sci Technol 2004, 38, 6475.
8. Carter, K. E.; Farrell, J. Separat Sci Technol 2010, 45, 762.
9. Hansen, M. C.; Borresen, M. H.; Schlabach, M.; Cornelissen, G. J Soil Sediment 2010, 10, 179.
10. Lipp, P.; Sacher, F.; Baldauf, G. Desalinat Water Treat 2010, 13, 226.
11. Steinle-Darling, E.; Reinhard, M. Environ Sci Technol 2008, 42, 5292.
12. Steinle-Darling, E. K.; Reinhard, M. Abstr Am Chem Soc 2008, 235, 64.
13. Tang, C. Y. Y.; Fu, Q. S.; Criddle, C. S.; Leckie, J. O. Environ Sci Technol 2007, 41, 2008.
14. Tang, C. Y. Y.; Fu, Q. S.; Robertson, A. P.; Criddle, C. S.; Leckie, J. O. Environ Sci Technol 2006, 40, 7343.
15. Tsai, Y. T.; Lin, A. Y. C.; Weng, Y. H.; Li, K. C. Environ Sci Technol 2010, 44, 7914.
16. Tang, C. Y. Y.; Kwon, Y. N.; Leckie, J. O. J Membr Sci 2007, 287, 146.
17. Tang, C. Y. Y.; Kwon, Y. N.; Leckie, J. O. Desalination 2009, 242, 149.
18. Tang, C. Y. Y.; Kwon, Y. N.; Leckie, J. O. Desalination 2009, 242, 168.
19. Manne, S.; Cleveland, J. P.; Gaub, H. E.; Stucky, G. D.; Hansma, P. K. Langmuir 1994, 10, 4409.
20. Manne, S.; Gaub, H. E. Science 1995, 270, 1480.
21. Wolgemuth, J. L.; Workman, R. K.; Manne, S. Langmuir 2000, 16, 3077.
22. Grosse, I.; Estel, K. Colloid Polym Sci 2000, 278, 1000.
23. Jaschke, M.; Butt, H. J.; Gaub, H. E.; Manne, S. Langmuir 1997, 13, 1381.
24. Wanless, E. J.; Ducker, W. A. J Phys Chem 1996, 100, 3207.
25. Shah, K.; Chiu, P.; Sinnott, S. B. J Colloid Interface Sci 2006, 296, 342.
26. Dominguez, H. J Phys Chem B 2007, 111, 4054.
27. Lampert, D. J.; Frisch, M. A.; Speitel, Jr., G. E. Pract Periodic Hazard Toxic Radioact Waste Manage 2007, 11, 60.
28. Moroi, Y.; Yano, H.; Shibata, O.; Yonemitsu, T. Bull Chem Soc Japan 2001, 74, 667.
29. Canadian Environmental Modelling Network, Newsletter, Editor: Webster, E., Spring 2006.
30. Stumm, W.; Morgan, J. Aquatic Chemistry; Wiley-Interscience: Hoboken, NJ, 1996.
31. Laughlin, R. G. In Advances in Liquid Crystals; Brown, G. H., Ed.; Academic Press: New York, 1978.
32. Belfer, S.; Purinson, Y.; Kedem, O. Acta Polymerica 1998, 49, 574.
33. Skrovanek, D. J.; Howe, S. E.; Painter, P. C.; Coleman, M. M. Macromolecules 1985, 18, 1676.
34. Silverstein, R. M.; Webster, F. X.; Kiemle, D. Spectrometric Identification of Organic Compounds; John Wiley: New York, 2005.
35. Socrates, G. Infrared Characteristic Group Frequencies; Wiley-Interscience: Hoboken, NJ, 1994.
36. Puro, L.; Manttari, M.; Pihlajamaki, A.; Nystrom, M. Chem Eng Res Des 2006, 84, 87.
37. Sadtler, The Infrared Spectra Atlas of Monomers and Polymers; Sadtler Research Laboratories, 1980.
38. Cheryan, M., Ed. Ultrafiltration and Microfiltration Handbook; CRC: Boca Raton, 1998.
39. Rosen, M. J. Surfactants and Interfacial Phenomena; Wiley: New York, 2004.
40. Higgins, C. P.; Luthy, R. G. Environ Sci Technol 2006, 40, 7251.